Structure of ^{43}Sc in the $\alpha+^{39}$K cluster model

Toshimi Sakuda
Department of Physics, Miyazaki University, Miyazaki 889-2155, Japan

Shigeo Ohkubo
Department of Applied Science, Kochi Women's University, Kochi 780-0844, Japan

(Received 25 August 1997)

The structure of ^{43}Sc is investigated by the $\alpha+^{39}$K orthogonality condition model. The properties investigated are energy spectra, α-spectroscopic factors, $E2$, $M1$, and $E1$ transitions. On the whole, the calculated properties are in good agreement with the available experimental data. Low-lying levels are assigned to the weak coupling multiplets based on $\alpha+^{39}$K$(3/2^+)$ and $\alpha+^{39}$K$(1/2^+)$ cluster configurations and interesting selectivities for $M1$ and $E1$ transitions are discussed. [S0556-2813(98)01103-0]

PACS number(s): 21.60.Gx, 27.40.+z, 23.20.−g, 21.10.−k

I. INTRODUCTION

There is continuing interest in the possibility that α-cluster structure persists in nuclei of the fp-shell region [1–8]. In the ^{40}Ca and ^{44}Ti nuclei the parity-doublet α-cluster bands and also the higher nodal states were observed by the α-transfer experiments [9–12]. In view of these facts we can say that the fp-shell nuclei would provide very fruitful grounds for studying α-cluster structure. Therefore, we have performed microscopic α-cluster model calculations with the orthogonality condition model (OCM) for the ^{40}Ca and ^{42}Ca nuclei [8]. Introducing cluster concept has the advantage of assisting our physical insight and making our calculations simpler. It has been shown that the α-cluster model is successful in accounting for the energy spectra, electromagnetic transitions and α-spectroscopic factors. Furthermore, the coexistence of α-cluster states and shell-model like states is essential to an understanding the structure of these nuclei.

For odd-A nuclei in the fp-shell region, the possible $4p$-mh intruder states candidates are not difficult to point out, since they have positive-parity contrary to $(fp)^n$ ground states. These have been pointed out by shell model analyses. However, α-clustering aspects of the intruder states are not yet confirmed. It would be very interesting to know if α-cluster structure is extended successfully to odd-A nuclei in which the symmetry breaking due to spin-orbit force would be stronger. It posseses great significance to investigate systematically the structure of the fp-shell nuclei including odd-A nuclei, in order to confirm that the α-cluster structure is a stable feature in this region.

The nucleus ^{43}Sc is very much the analogue in the fp-shell of ^{19}F in the sd-shell, and provides the first link in the chain of α-mh cluster states in $A=44-40$ nuclei. It should provide a good testing ground for looking at the persistence of α-cluster structure in heavy nuclei. It is also interesting to investigate the trace of an analogy between the ^{43}Sc and ^{19}F nuclei [13]. Although there are no reported α-transfer data for the nucleus ^{43}Sc, many data on the spectroscopy and electromagnetic properties may be helpful in making assignments of α-cluster states. The most striking feature is that the lowest $3/2^+$ level is located at extremely low-excitation energy ($E_x=0.15$ MeV), which cannot be described in terms of the simple shell model [14]. Some measured $E2$-transitions of the positive-parity states show strong enhancement comparable to those of α-cluster bands in ^{40}Ca and ^{44}Ti. These suggest that the nucleus ^{43}Sc might well contain a low-lying positive-parity band of states having the $\alpha+^{39}$K cluster structure.

The classification of the band structure, however, is still not so clear cut. A weak coupling interpretation lead one to expect to find low-lying states which can be described as the $3/2^+$ spin of ^{39}K couples to the relative angular momentum of α [15,7,3]. Noncentral parts of the α-^{39}K interaction seem to break the degeneracy of the quadruplets in a slightly complicated manner. Alternatively, one may consider these levels as two rotational bands built on deformed intrinsic states with $K^\pi=3/2^+$ and $K^\pi=1/2^+$ [14].

We report here on a study of ^{43}Sc by microscopic $\alpha+^{39}$K OCM, which is essentially the same approach as ^{40}Ca and ^{42}Ca in Ref. [8]. We analyze the energy spectra, the wave functions, α-spectroscopic factors, and electromagnetic transitions.

II. ORTHOGONALITY CONDITION MODEL FOR $\alpha+^{39}$K SYSTEM

The model space of the $\alpha+^{39}$K cluster model is described by a set of the wave functions

$$\Psi_J=\frac{\mathcal{A}}{\sqrt{\binom{43}{4}}}\{\phi(\alpha)[\phi_I(^{39}\mathrm{K})Y_l(\hat{\mathbf{r}})]_J R_{Nl}(r)\}, \qquad (1)$$

where $\mathcal{A}$ is the antisymmetrizer between α and ^{39}K and $R_{Nl}(r)$ is a radial harmonic oscillator wave function with N oscillator quanta for the relative motion. The antisymmetrized internal wave functions $\phi(\alpha)$ and $\phi_I(^{39}\mathrm{K})$ are assumed to be shell-model $(0s)^4$ and $(sd)^{-1}(\lambda\mu)=(02)$ configurations, respectively, with a common oscillator parameter $a=0.2815$ fm^{-2}. The angular momenta of ^{39}K and the relative motion, I and l, are coupled to the total angular momentum J. The model space is generated as a direct product of

TABLE I. SU(3) classification of the allowed states of $\alpha+^{39}$K system.

N	(λ,μ)		
11	(9,0)		
12	(12,2)	(11,1)	(10,0)
13	(13,2)	(12,1)	(11,0)
14	(14,2)	(13,1)	(12,0)
⋮	⋮	⋮	⋮
N	$(N,2)$	$(N-1,1)$	$(N-2,0)$

the internal wave functions and the relative ones: $(02)\times(N0)$. Furthermore, the model space is classified by SU(3) symmetry. Table I lists the SU(3) label $(\lambda\mu)$ for the Pauli-allowed states. The states with $N<11$ are not allowed due to the Pauli principle. It is worth while noting that the present model space contains many important shell-model states such as the $3p$ state (9,0) and the $4p$-$1h$ state (12,2). In the present calculation, we make a truncation of the model space: the total oscillator quanta $N=11$–30 and the relative angular momentum $l=0$–16, which can guarantee energy convergence of the low-lying states of ^{43}Sc.

The Hamiltonian of the system is written as

$$H=H(\alpha)+H(^{39}\mathrm{K})+T_{\alpha\text{-K}}+V_{\alpha\text{-K}}, \tag{2}$$

where $H(\alpha)$ and $H(^{39}\mathrm{Kr})$ are the internal Hamiltonians for α and ^{39}K and $T_{\alpha\text{-K}}$ is the kinetic energy operator for the relative motion. The excitation energies of the $1/2^+$ and $5/2^+$ states of ^{39}K are suggested by the observed spectrum as 2.5 MeV and 5.8 MeV, respectively.

The intercluster potential $V_{\alpha\text{-K}}$ is taken to be a folding potential after the one used in Ref. [8], namely,

$$V_{\alpha\text{-K}}=V^C+V^I\boldsymbol{I}^2+V^{T2}[T_2,Y_2]_0+V^{T2'}[T'_2,Y_2]_0 +V^{T4}[T_4,Y_4]_0, \tag{3}$$

where

$$T_{\lambda\mu}=\sum_{i\in\mathrm{K}} y_{\lambda\mu}(\boldsymbol{\xi}_i), \quad T'_{2\mu}=\sum_{i\in\mathrm{K}} \xi_i^2 y_{2\mu}(\boldsymbol{\xi}_i), \tag{4}$$

and $\boldsymbol{I}$ is the angular momentum of ^{39}K. The nucleon-nucleon interaction adopted is the Hasegawa-Nagata-Yamamoto force [16] with depth parameter $V_0(^3E)=-493$ MeV for the intermediate range. As for the Coulomb interaction, only the central part is adopted, and the tensor parts derived from the Coulomb force are very small and are neglected. The depths V^{T2} and $V^{T2'}$ are multiplied by factors 1.1 and 0.9, respectively, so as to reproduce the low-lying states energies; these factors are similar to those used in the ^{40}Ca and ^{42}Ca systems, but are more moderate.

A. Energy spectra

The calculated energy spectra are compared with the experimental data in Fig. 1, where the energies are given with respect to the $\alpha+^{39}$K threshold ($E_{\mathrm{th}}=4.81$ MeV) and the label of the total angular momentum denotes $2\times J$ value.

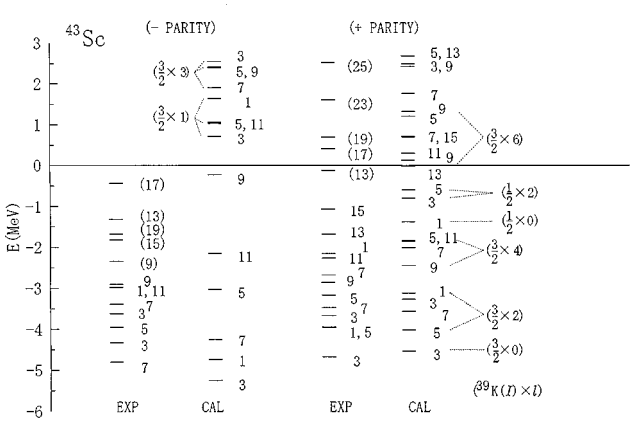

FIG. 1. Calculated and experimental energy spectra of ^{43}Sc. The energy scale is measured from the α-threshold and the label of the total angular momentum denotes $2\times J$ value. The multiplets of $[^{39}\mathrm{K}(I)\times l]$ cluster band are indicated by dotted lines. Experimental energies are from Refs. [17,18].

In the negative-parity states, the agreement with the experiment is not so good. This is probably ascribed to the restricted basis of the present model that includes only the (90) configuration in the lowest $(fp)^3$ space and does not consider the spin-orbit splittings of single-particle orbits. The admixture with $(fp)^3$ configurations other than (90) is needed to yield good agreement. Furthermore, it is said that the states $3/2^-_1$ ($E_x=0.47$ MeV), $5/2^-_1$ (0.85 MeV) and $7/2^-_2$ (1.42 MeV) could not be accounted for using shell model calculations with $(fp)^3$ configuration [14,19]. It is also important to consider the mixing with core-excited configurations in order to improve the agreement. On the other hand, the triton transfer reaction data show that many of low-lying negative-parity states are strongly populated [20]. Also, according to the shell model calculation [21], the (90) component is maintained to amount of 30–50% in many of the low-lying states. These could be interpreted to indicate the trace of triton cluster structure of the states.

The negative-parity band with the $\alpha+^{39}\mathrm{K}(3/2^+)$ cluster structure is predicted to start at 0.78 MeV above the α-threshold. This is a close analogue of the negative-parity α-cluster bands in the neighboring nuclei. It is very important to search for the experimental candidates of the α-cluster bands.

As for the positive-parity states, agreement with the experiment is very fine. The spin sequence of low-lying levels can be interpreted in terms of weak coupling scheme built on $[^{39}\mathrm{K}(3/2^+$ or $1/2^+)\times l]$, as depicted in Fig. 1. The lowest band is dominated by the $[^{39}\mathrm{K}(3/2^+)\times l]$ configuration. The second-rank tensor forces produce a fairly large splitting of the lowest band into quadruplets, which looks different from a very small splitting of the lowest band $[^{15}\mathrm{N}(1/2^-)\times l]$ in the ^{19}F nucleus. The angular momenta of $^{39}\mathrm{K}(3/2^+)$ and $^{15}\mathrm{N}(1/2^-)$ are mainly responsible for the features of splittings. The second-rank tensor forces cannot produce the splitting of the band $[^{15}\mathrm{N}(1/2^-)\times l]$ because of angular momentum selection rule. The strengths of the tensor forces are not much different in both nuclei. Then, the basic weak coupling feature remains unchanged. The excited band $[^{39}\mathrm{K}(1/2^+)\times l]$ is predicted to be built on the $1/2^+_2$ state. The

TABLE II. Wave functions of the negative-parity states in terms of the SU(3) scheme.

		$N=11$	$N=13$					
		$L=odd$	$L=odd$				$L=even$	
J^π	E (MeV)	(9,0)	$(13,2)_1$	$(13,2)_2$	(12,1)	(11,0)	(13,2)	(12,1)
$1/2^-$	-4.66	0.915	0.026		-0.068	-0.187		
$1/2^-$	1.71	-0.130	-0.436		-0.492	-0.126		
$3/2^-$	-5.18	0.922	0.030		0.013	-0.181	-0.004	-0.042
$3/2^-$	0.78	-0.025	-0.069		-0.187	-0.021	-0.634	-0.174
$5/2^-$	-2.96	0.914	-0.013	0.017	0.082	-0.190	0.005	0.036
$5/2^-$	1.13	-0.087	0.302	0.490	0.274	-0.044	0.229	-0.078
$7/2^-$	-4.17	0.931	-0.029	0.004	-0.003	-0.175	0.006	0.035
$7/2^-$	1.97	0.038	-0.046	0.315	-0.138	0.036	-0.560	-0.211
$9/2^-$	-0.15	0.912	-0.016	0.034	0.112	-0.192	0.020	0.047
$9/2^-$	2.46	-0.164	-0.015	0.537	0.301	-0.044	0.278	0.009
$11/2^-$	-2.08	0.943	-0.021	-0.015	0.007	-0.168	0.007	0.030
$11/2^-$	4.05	0.041	-0.298	0.219	-0.123	0.043	-0.546	-0.209

observed $1/2_2^+$ (2.65 MeV) is a good candidate for this state. There are some problems associated with the spectrum. The $1/2_1^+$ state is calculated about 0.8 MeV higher than the experimental $1/2_1^+$ (0.85 MeV) state. Moreover, the higher spin states ($\geqslant 17/2^+$) are predicted to lie at too high excitation energies and are not shown in Fig. 1. The systematic deviations of the upper levels from the rotational spectrum are also observed in the α-cluster bands of ^{40}Ca and ^{44}Ti. To overcome these difficulties, the present model may be developed to include the symmetry breaking of α-cluster states [22].

B. Wave functions and α-spectroscopic factors

The calculated wave functions of the negative-parity states in terms of the SU(3) scheme are listed in Table II, where the LS coupling scheme is used and the total orbital angular momentum $L=|J-1/2|$ or $J+1/2$. The components of quanta higher than $N=13$ are abbreviated. The bases with the same $(\lambda\mu)$ but different K labels are not orthogonal with respect to K, which refers to the component of the orbital angular momentum along the intrinsic z-axis. Therefore, we make a set of orthogonal bases by diagonalizing the norm kernel; the bases $(13,2)_1$ and $(13,2)_2$ are such functions. The

TABLE III. Wave functions of the positive-parity states in terms of the SU(3) scheme.

		$N=12$						$N=14$					
		$L=even$				$L=odd$		$L=even$				$L=odd$	
J_i^π	E (MeV)	$(12,2)_1$	$(12,2)_2$	(11,1)	(10,0)	(12,2)	(11,1)	$(14,2)_1$	$(14,2)_2$	(13,1)	(12,0)	(14,2)	(13,1)
$1/2_1^+$	-3.11	0.537			-0.210		-0.590	-0.218			0.083		0.242
$1/2_2^+$	-1.37	0.586			0.436		0.364	-0.247			-0.186		-0.151
$3/2_1^+$	-4.52	0.671	-0.384	0.249	-0.048		0.184	-0.262	0.153	-0.102	0.019		-0.074
$3/2_2^+$	-3.27	-0.331	-0.396	0.483	-0.204		-0.373	0.129	0.160	-0.199	0.082		0.152
$3/2_3^+$	-0.79	0.226	0.585	0.319	-0.388		-0.162	-0.096	-0.244	-0.136	0.166		0.067
$5/2_1^+$	-4.01	-0.319	0.002	0.186	-0.045	0.714	0.231	0.124	-0.001	-0.075	0.018	-0.279	-0.093
$5/2_2^+$	-1.82	-0.174	-0.597	-0.367	-0.140	-0.117	0.373	0.073	0.243	0.150	0.052	0.044	-0.151
$5/2_3^+$	-0.58	-0.168	-0.457	0.255	0.482	0.019	-0.374	0.070	0.193	-0.102	-0.201	-0.004	0.152
$7/2_1^+$	-3.56	-0.622	-0.261	-0.349	0.085	-0.332	0.038	0.260	0.059	0.143	-0.034	0.130	-0.014
$7/2_2^+$	-1.99	0.314	-0.441	-0.349	0.166	0.159	-0.482	-0.083	0.192	0.143	-0.065	-0.059	0.193
$7/2_3^+$	0.71	-0.008	0.636	-0.333	0.357	-0.038	-0.210	-0.043	-0.257	0.142	-0.150	0.016	0.087
$9/2_1^+$	-2.44	0.396	-0.153	-0.157	0.058	-0.670	-0.241	-0.139	0.084	0.062	-0.022	0.260	0.095
$11/2_1^+$	-1.85	0.291	-0.591	-0.362	0.085	0.360	0.035	-0.112	0.237	0.147	-0.032	-0.141	-0.014
$13/2_1^+$	-0.00	-0.463	0.077	-0.152	0.060	0.664	0.226	0.172	-0.033	0.059	-0.021	-0.252	-0.085
$15/2_1^+$	0.70	-0.238	0.632	0.339	-0.067	-0.379	-0.066	0.090	-0.250	-0.134	0.023	0.145	0.024
$17/2_1^+$	3.31	0.500	-0.073	0.156	-0.054	-0.676	-0.195	-0.174	0.035	-0.057	0.016	0.243	0.067
$19/2_1^+$	4.15	0.222	-0.673	-0.294	0.040	0.403	0.073	-0.079	0.257	0.108	-0.011	-0.147	-0.023
$21/2_1^+$	7.49	-0.539	0.051	-0.167	0.415	0.700	0.145	0.167	-0.031	0.054	-0.008	-0.225	-0.042
$23/2_1^+$	8.50	0.722	0.219	0.227		-0.436	-0.063	0.073	-0.250	-0.069	0.000	0.144	0.015
$25/2_1^+$	12.50	0.004	0.582	-0.183		-0.732		0.139	-0.021	0.046	0.003	-0.181	-0.008
$27/2_1^+$	13.70	-0.815				0.481		-0.209	-0.065	-0.012		0.122	-0.001

TABLE IV. Spectroscopic factors S_α^2 of $\alpha+^{39}\mathrm{K}(I^\pi=1/2^+,3/2^+,5/2^+)$ channels for the negative parity states.

J^π	E (MeV)	channel ($I\times l$)					
		$(1/2\times1)$	$(3/2\times1)$		$(5/2\times3)$		
$1/2^-$	-4.66	0.047	0.048		0.059		
$1/2^-$	1.70	0.050	0.334		0.002		
		$(1/2\times1)$	$(3/2\times1)$	$(3/2\times3)$	$(5/2\times1)$	$(5/2\times3)$	
$3/2^-$	-5.18	0.045	0.004	0.050	0.025	0.023	
$3/2^-$	0.78	0.001	0.367	0.008	0.001	0.000	
		$(1/2\times3)$	$(3/2\times1)$	$(3/2\times3)$	$(5/2\times1)$	$(5/2\times3)$	$(5/2\times5)$
$5/2^-$	-2.96	0.044	0.025	0.018	0.001	0.006	0.058
$5/2^-$	1.13	0.004	0.307	0.065	0.000	0.001	0.001
		$(1/2\times3)$	$(3/2\times3)$	$(3/2\times5)$	$(5/2\times1)$	$(5/2\times3)$	$(5/2\times5)$
$7/2^-$	-4.17	0.041	0.006	0.053	0.011	0.012	0.017
$7/2^-$	1.97	0.002	0.364	0.006	0.001	0.000	0.000
		$(1/2\times5)$	$(3/2\times3)$	$(3/2\times5)$	$(5/2\times3)$	$(5/2\times5)$	$(5/2\times7)$
$9/2^-$	-0.15	0.035	0.031	0.013	0.001	0.006	0.063
$9/2^-$	2.46	0.006	0.332	0.029	0.001	0.001	0.002
		$(1/2\times5)$	$(3/2\times5)$	$(3/2\times7)$	$(5/2\times3)$	$(5/2\times5)$	$(5/2\times7)$
$11/2^-$	-2.08	0.033	0.006	0.057	0.008	0.009	0.017
$11/2^-$	4.05	0.002	0.357	0.003	0.001	0.000	0.000

first state of each J is dominated by the (90) of $3p$ configurations and contains some of the (11,0) configuration. The (90) component of the $1/2_1^-$ state is about 84%, which is somewhat larger than the lowest (60) component (74%) of the $1/2_1^+$ state in ^{19}F. This means that the t-clustering in ^{43}Sc becomes weaker than in ^{19}F [13]. The second state of each J is somewhat complicated. They appear to contain appreciable higher components like (13,2) and (12,1), and are expected to be $\alpha+^{39}\mathrm{K}(3/2^+)$ cluster states. It is of significance to search for the experimental candidates of the negative-parity α-cluster bands.

The calculated wave functions of the positive-parity states in terms of the SU(3) scheme are also shown in Table III. The components of quanta higher than $N=14$ are abbreviated. These states are substantial mixtures of (12,2), (11,1) and (10,0) configurations in the lowest quanta. This is the result of the product of the internal wave functions and relative ones: $(0,2)\times(12,0)$. The same kind of feature is also held in $N=14$ case. Therefore these states can be viewed as $\alpha+^{39}$K cluster states. The lowest $3/2_1^+$ state has a 69% component with the lowest quanta, which is somewhat larger than the corresponding component (56%) of the lowest $1/2_1^-$ state in ^{19}F. The smaller mixture of higher components in ^{43}Sc indicates that the degree of α-clustering becomes weaker in ^{43}Sc than in ^{19}F.

Although there are no reported α-transfer data for ^{43}Sc, a decomposition of the wave functions into channel components would be interesting. The spectroscopic factors S_α^2 of the $\alpha+^{39}\mathrm{K}(I^\pi=1/2^+,3/2^+,5/2^+)$ channels are listed in Tables IV and V. As for the negative-parity states, the S_α^2 factors of the lowest states are about 0.04 in most channels. This is due to a nonorthogonality of channel wave functions with low-oscillator quanta. The second state of each J has a large S_α^2 factor (about 0.3) in $(3/2^+\times l)$ channel and is a well developed α-cluster state. These features are clearly illustrated in Fig. 2, which shows reduced width amplitudes (RWA's), $y(r)$, of the $3/2_1^-$ and $3/2_2^-$ states for the $^{39}\mathrm{K}(3/2^+$, or $1/2^+)+\alpha$ channels.

The low-lying positive-parity states have a large S_α^2 factor (about 0.18) in $(3/2\times l)$ channel and are the members of $\alpha+^{39}\mathrm{K}(3/2^+)$ cluster band. Similarly, the states $1/2_2^+$, $3/2_3^+$, $5/2_3^+$, ... have a large S_α^2 factor in $(1/2\times l)$ channel and are largely $\alpha+^{39}\mathrm{K}(1/2^+)$ cluster states. All of the S_α^2 factors in $(5/2\times l)$ channel are found to be very small in these states. These results confirm the weak coupling feature of $\alpha+^{39}$K cluster bands. The features of various α-cluster channels of the lowest three $3/2^+$ states are illustrated in Fig. 3. The heights of the outermost peaks of the RWA's are greatly enhanced and show the importance of α-clustering. The typical value (0.18) of S_α^2 factor of α-cluster states in ^{43}Sc is somewhat smaller than the corresponding S_α^2 factor (0.3) in ^{19}F. This value, however, is still much larger than the S_α^2 factor (0.071) of the $4p$-$1h$ (12,2) state in SU(3) shell model, and is as large as the values of α-cluster sates in ^{40}Ca and ^{42}Ca nuclei. We can say that the α-clustering structure still persists in the ^{43}Sc nucleus.

C. Electromagnetic transitions and moments

We can calculate the electromagnetic transitions in a microscopic way by using the knowledge of the norm kernel, which is the same method as used in the previous calculations of ^{40}Ca and ^{42}Ca [8]. The transition matrix elements of the subunit cluster ^{39}K is calculated by using the SU(3) shell model wave functions. The details of the calculational method are given in Ref. [13].

Calculated and observed $B(E2)$ and $B(M1)$ values are summarized in Tables VI and VII. In the calculation of $E2$ transitions, additional charges $\delta e_p=\delta e_n=0.3e$ for the internal transitions of ^{39}K are used in order to reproduce the experimental $B[E2:1/2^+(2.52\ \mathrm{MeV})\rightarrow3/2^+(0.0\ \mathrm{MeV})]$ value, and small additional charges $\delta e_p=\delta e_n=0.1e$ for the

TABLE V. Spectroscopic factors S_α^2 of $\alpha+{}^{39}\mathrm{K}(I^\pi=1/2^+,3/2^+,5/2^+)$ channels for the positive parity states.

J_i^π	E (MeV)	channel ($I\times l$)					
		$(1/2\times0)$	$(3/2\times2)$		$(5/2\times2)$		
$1/2_1^+$	-3.11	0.026	0.176		0.001		
$1/2_2^+$	-1.38	0.184	0.045		0.004		
		$(1/2\times2)$	$(3/2\times0)$	$(3/2\times2)$	$(5/2\times2)$	$(5/2\times4)$	
$3/2_1^+$	-4.52	0.001	0.143	0.044	0.001	0.000	
$3/2_2^+$	-3.27	0.011	0.049	0.142	0.000	0.001	
$3/2_3^+$	-0.79	0.197	0.009	0.013	0.001	0.002	
		$(1/2\times2)$	$(3/2\times2)$	$(3/2\times4)$	$(5/2\times0)$	$(5/2\times2)$	$(5/2\times4)$
$5/2_1^+$	-4.01	0.001	0.181	0.003	0.001	0.000	0.001
$5/2_2^+$	-1.82	0.062	0.002	0.125	0.001	0.001	0.000
$5/2_3^+$	-0.58	0.139	0.005	0.084	0.004	0.003	0.001
		$(1/2\times4)$	$(3/2\times2)$	$(3/2\times4)$	$(5/2\times2)$	$(5/2\times4)$	$(5/2\times6)$
$7/2_1^+$	-3.56	0.001	0.166	0.021	0.001	0.001	0.000
$7/2_2^+$	-1.99	0.007	0.026	0.157	0.000	0.000	0.001
$7/2_3^+$	0.71	0.190	0.007	0.009	0.002	0.001	0.001
		$(1/2\times4)$	$(3/2\times4)$	$(3/2\times6)$	$(5/2\times2)$	$(5/2\times4)$	$(5/2\times6)$
$9/2_1^+$	-2.44	0.001	0.176	0.002	0.001	0.000	0.001
$9/2_2^+$	0.13	0.130	0.000	0.047	0.003	0.001	0.000
$9/2_3^+$	1.32	0.052	0.004	0.148	0.014	0.001	0.001
		$(1/2\times6)$	$(3/2\times4)$	$(3/2\times6)$	$(5/2\times4)$	$(5/2\times6)$	$(5/2\times8)$
$11/2_1^+$	-1.85	0.001	0.175	0.009	0.001	0.000	0.000
$11/2_2^+$	0.29	0.006	0.012	0.156	0.000	0.000	0.000
$11/2_3^+$	3.08	0.154	0.004	0.008	0.024	0.001	0.001
		$(1/2\times6)$	$(3/2\times6)$	$(3/2\times8)$	$(5/2\times4)$	$(5/2\times6)$	$(5/2\times8)$
$13/2_1^+$	-0.00	0.001	0.165	0.001	0.001	0.000	0.000
$13/2_2^+$	2.68	0.148	0.001	0.010	0.015	0.001	0.000
		$(1/2\times8)$	$(3/2\times6)$	$(3/2\times8)$	$(5/2\times6)$	$(5/2\times8)$	$(5/2\times10)$
$15/2_1^+$	0.70	0.001	0.169	0.004	0.001	0.000	0.000
$15/2_2^+$	3.50	0.006	0.006	0.141	0.001	0.000	0.000
		$(1/2\times8)$	$(3/2\times8)$	$(3/2\times10)$	$(5/2\times6)$	$(5/2\times8)$	$(5/2\times10)$
$17/2_1^+$	3.31	0.002	0.147	0.001	0.001	0.000	0.001
		$(1/2\times10)$	$(3/2\times8)$	$(3/2\times10)$	$(5/2\times8)$	$(5/2\times10)$	$(5/2\times12)$
$19/2_1^+$	4.15	0.001	0.153	0.003	0.001	0.000	0.000
		$(1/2\times10)$	$(3/2\times10)$	$(3/2\times12)$	$(5/2\times8)$	$(5/2\times10)$	$(5/2\times12)$
$21/2_1^+$	7.49	0.002	0.123	0.001	0.002	0.000	0.000
		$(1/2\times12)$	$(3/2\times10)$	$(3/2\times12)$	$(5/2\times10)$	$(5/2\times12)$	$(5/2\times14)$
$23/2_1^+$	8.50	0.001	0.130	0.002	0.001	0.000	0.000
		$(1/2\times12)$	$(3/2\times12)$	$(3/2\times14)$	$(5/2\times10)$	$(5/2\times12)$	$(5/2\times14)$
$25/2_1^+$	12.50	0.003	0.094	0.000	0.001	0.000	0.000
		$(1/2\times14)$	$(3/2\times12)$	$(3/2\times14)$	$(5/2\times12)$	$(5/2\times14)$	$(5/2\times16)$
$27/2_1^+$	13.71	0.001	0.100	0.001	0.001	0.000	0.000

relative transitions are also used, which are consistent with the values needed in the calculations of ${}^{40}\mathrm{Ca}\sim{}^{44}\mathrm{Ti}$ [8]. These are far smaller than the additional charges used in the shell-model calculation [19,24], which are $\delta e_p=0.4e$ and $\delta e_n=0.6e$ for negative-parity and further $\delta e_p=2.5e$ and $\delta e_n=1.5e$ for positive-parity states.

For the $E2$ transitions from the high-spin ($J^\pi=19/2^-,15/2^-,11/2^-$ and $9/2^-$) states, the calculated and experiments are in agreement. While for $J^\pi=3/2^-,5/2^-$ case, two neighboring levels are observed and both have relatively strong $E2$ transitions. As mentioned before, the present model can predict only one state of each J in this energy region. The calculated $B(E2)$ value, however, is comparable with the experimental values. In view of these facts we can say that the (90) strength is shared over the two states and admixtures of core-excited components into these states are important. For the $M1$ transitions we use the free charge and gyromagnetic ratios. In the cluster model, the $M1$ operator cannot change the total orbital angular momentum L and thus $M1$ transition between states of $\Delta L=2$ should be forbidden. The $B(M1{:}3/2^-\rightarrow5/2^-)$ and $B(M1{:}9/2^-\rightarrow7/2^-)$ are such cases, and these are in fact observed to be very weak. On the other hand, $M1$ transitions with $\Delta L=0$ such as $B(M1{:}5/2^-\rightarrow7/2^-)$ and $B(M1{:}1/2^-$

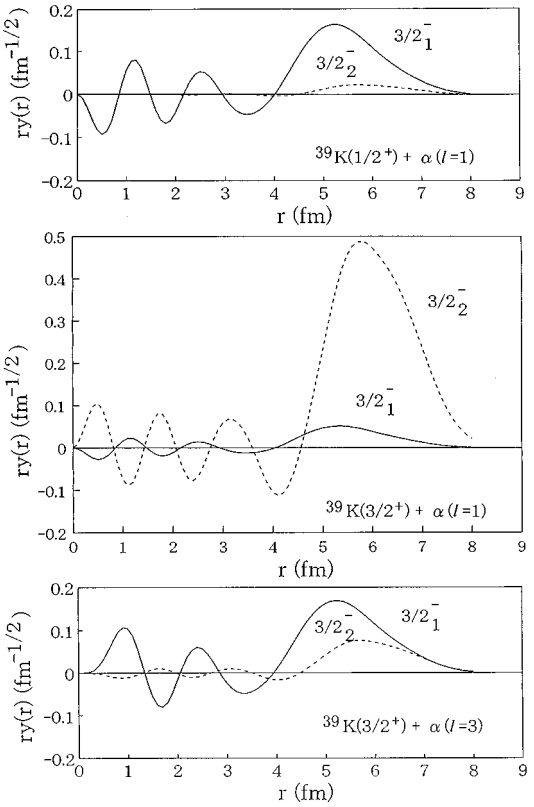

FIG. 2. The reduced width amplitudes of the $3/2^-$ states for the $^{39}\mathrm{K}(3/2^+)+\alpha$ and $^{39}\mathrm{K}(1/2^+)+\alpha$ channels.

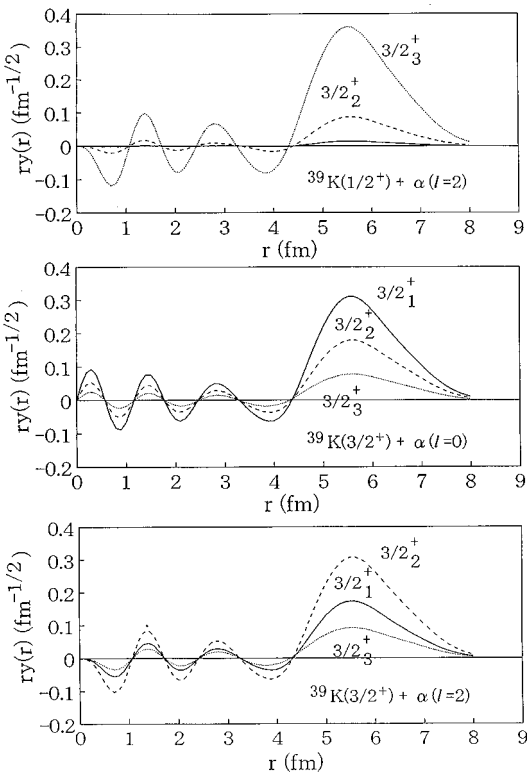

FIG. 3. The reduced width amplitudes of the $3/2^+$ states for the $^{39}\mathrm{K}(3/2^+)+\alpha$ and $^{39}\mathrm{K}(1/2^+)+\alpha$ channels.

$\rightarrow 3/2^-$) are allowed and are an order of magnitude larger than the transitions with $\Delta L=2$. The quadrupole moments of the $7/2^-$(0.0 MeV) and $19/2^-$(3.12 MeV) are also reasonably reproduced. The calculated magnetic moments of the states are somewhat smaller than the experimental values. This is due to lack of $(f_{7/2})^3$ components in the present wave functions.

As noted in the Introduction, the observed $E2$ transitions of the positive-parity states are strongly enhanced, and are reproduced very well by the present model. Furthermore, the $B[E2{:}3/2^+(1.16)\rightarrow 3/2^+(0.15)]$ is smaller than other inband transitions and shows some deviation from the simple weak coupling interpretation. This is also well explained by the present model. It is noteworthy that only small effective charge is used in the calculation. In the shell-model calculation, very large effective charges are commonly required. These enhancements are ascribed to the α-clustering of the states, which are very similar to the cluster model calculations in ^{40}Ca and ^{42}Ca. We are also able to obtain a good

TABLE VI. Calculated and experimental $E2$ and $M1$ transitions of negative-parity states in ^{43}Sc.

			Experimental [a]		Calculated	
$J^\pi_i(E^{\mathrm{ex}}_i)$	$\rightarrow$	$J^\pi_f(E^{\mathrm{ex}}_f)$	$B(E2)_{\mathrm{W.u.}}$	$B(M1)_{\mathrm{W.u.}}$	$B(E2)_{\mathrm{W.u.}}$	$B(M1)_{\mathrm{W.u.}}$
$3/2^-$(0.47)	$\rightarrow$	$7/2^-$(0.0)	16 ± 1			
$3/2^-$(1.18)	$\rightarrow$	$7/2^-$(0.0)	9 ± 3		13.41	
	$\rightarrow$	$5/2^-$(0.85)		<0.259		0.001
$1/2^-$(1.81)	$\rightarrow$	$3/2^-$(0.47)		$0.176\sim0.395$		
	$\rightarrow$	$3/2^-$(1.18)	$\ll 30000$	$3.1^{+1.5}_{-0.8}$	11.38	2.17
$5/2^-$(0.85)	$\rightarrow$	$7/2^-$(0.0)	15 ± 7 or 7 ± 3	0.114 ± 0.02		
$5/2^-$(2.29)	$\rightarrow$	$7/2^-$(0.0)	>0.03	>0.087	1.05	2.66
$11/2^-$(1.83)	$\rightarrow$	$7/2^-$(0.0)	13.6 ± 1.5		6.68	
$9/2^-$(1.88)	$\rightarrow$	$7/2^-$(0.0)	$1.6^{+1.1}_{-0.6}$	$0.057^{+0.034}_{-0.016}$	0.41	0.024
	$\rightarrow$	$5/2^-$(0.85)	<73		7.27	
$15/2^-$(2.92)	$\rightarrow$	$11/2^-$(1.83)	5.4 ± 0.6		5.24	
$19/2^-$(3.12)	$\rightarrow$	$15/2^-$(2.92)	2.82 ± 0.05		2.91	
			$Q(e\ \mathrm{fm}^2)$	μ(nm)	$Q(e\ \mathrm{fm}^2)$	μ(nm)
$7/2^-$(0.0)			-26 ± 6	4.61 ± 0.04	-16.17	1.74
$19/2^-$(3.12)			$\pm19.9\pm14$	3.121 ± 0.007	-17.06	1.53

[a]References [17,23–25].

TABLE VII. Calculated and experimental $E2$ and $M1$ transitions of positive-parity states in ^{43}Sc.

			Experimental [a]		Calculated	
$J_i^\pi(E_i^{ex})$	→	$J_f^\pi(E_f^{ex})$	$B(E2)_{W.u.}$	$B(M1)_{W.u.}$	$B(E2)_{W.u.}$	$B(M1)_{W.u.}$
$[^{39}K(3/2)\times l=2]$						
$5/2^+(0.88)$	→	$3/2^+(0.15)$	14 ± 4	0.011 ± 0.005	28.93	0.015
$3/2^+(1.16)$	→	$3/2^+(0.15)$	4.4 ± 1.5	$0.039^{+0.054}_{-0.026}$	1.01	0.010
$7/2^+(1.34)$	→	$3/2^+(0.15)$	19 ± 8		14.15	
	→	$5/2^+(0.88)$	31 ± 22	$0.030^{+0.014}_{-0.009}$	20.43	0.072
$[^{39}K(3/2)\times l=4]$						
$5/2^+(1.65)$	→	$1/2^+(0.86)$	35 ± 13		17.82	
	→	$3/2^+(1.16)$			6.98	0.100
$9/2^+(1.93)$	→	$5/2^+(0.88)$	16 ± 4		18.11	
	→	$7/2^+(1.34)$	4.1 ± 2.0	0.014 ± 0.005	8.56	0.019
$11/2^+(2.55)$	→	$7/2^+(1.34)$	31 ± 8		23.97	
	→	$9/2^+(1.93)$	21 ± 8	0.106 ± 0.018 or 0.23 ± 0.17	9.78	0.24
$[^{39}K(3/2)\times l=10]$						
$23/2^+(6.43)$	→	$19/2^+(5.52)$	5.6 ± 0.5		15.86	
$[^{39}K(3/2)\times l=12]$						
$25/2^+(7.36)$	→	$23/2^+(6.43)$	<2	0.07 ± 0.05	0.23	0.001
			$Q(e\ fm^2)$	μ(nm)	Q(e fm^2)	μ(nm)
$3/2^+(0.15)$				0.348 ± 0.006	18.83	0.214

[a]References [17,24–27].

account of the $M1$ transitions. In the α-cluster states, only the transition between states of $\Delta l=0$ should be allowed, which is the same kind of selection rule as the one in the negative-parity states. As can be seen from the Table VII, there are a number of such transitions, for example, $B[M1:11/2^+(2.55)\rightarrow 9/2^+(1.93)]$. These are much larger than the forbidden transitions between the states of $\Delta l=2$. Moreover, the calculated magnetic moment of the $3/2^+(0.15)$ is also in reasonable agreement with the observed value.

As the present cluster model contains no spurious center-of-mass excitation, we can treat $E1$ transitions without anxiety. The calculated and experimental $E1$ transitions are given in Table VIII. The present α-cluster model gives a good account of the $E1$ transitions, also. In this calculation, no effective charge is used. An interesting feature of the transitions was noticed in Ref. [23]. That is, the observed strengths related to $K^\pi=3/2^+$ band are all hindered by $\simeq 10^5$ and the ones related to the $K^\pi=1/2^+$ band are all hindered by $\simeq 10^4$. Since the $E1$ operator transforms as $(\lambda\mu)=(10)$ under SU(3), there are severe constraints on the $E1$ transitions from $(fp)^3$ (90) states to $4p$-$1h$ states: the transition to (10,0) is allowed but the ones to (12,2) or (11,1) states are forbidden. The (10,0) configuration is only a small component of the low-lying positive-parity states and that the $E1$ transitions between the $(fp)^3$ and $4p$-$1h$ states should be greatly inhibited. As shown in Table III, the (10,0) components of the $3/2^+_1$, $5/2^+_1$ and $7/2^+_1$ states, which look like members of $K^\pi=3/2^+$ band, are considerably smaller than the ones of the $1/2^+_1$, $3/2^+_2$ and $5/2^+_2$ states, which look like members of $K^\pi=1/2^+$ band. This is a reason for the variety of hindrances of the $E1$ transitions. It is known that the $E1$ transition rates are influenced by the giant dipole resonance. The excitation energy of the giant dipole resonance peak is about 70 MeV, which is far larger than the energy gap of the concerned levels. Therefore, the effect would have a small state dependence and is not expected to explain the large difference of the observed retardations of the $E1$ transitions. As a whole, these lend strong supports to the present interpretation of ^{43}Sc.

TABLE VIII. Calculated and experimental $E1$ transitions in ^{43}Sc.

			$B(E1)$(W.u.$\times10^{-5}$)	
$J_i^\pi(E_i^{ex})$	→	$J_f^\pi(E_f^{ex})$	Experimental [a]	Calculated
$3/2^-(0.47)$	→	$3/2^+(0.15)$	0.4 ± 0.2	0.27
$5/2^-(0.85)$	→	$3/2^+(0.15)$	<25	2.10
$5/2^+(0.88)$	→	$7/2^-(0.0)$	0.4 ± 0.2	1.42
$1/2^+(0.86)$	→	$3/2^-(0.47)$	13 ± 4	27.7
$3/2^+(1.16)$	→	$5/2^-(0.85)$	<20	32.7
$7/2^+(1.34)$	→	$7/2^-(0.0)$	$3.3^{+1.0}_{-0.7}$	0.24
$5/2^+(1.65)$	→	$7/2^-(0.0)$	25 ± 9	6.69
	→	$3/2^-(0.47)$	11 ± 4	5.56

[a]Reference [23].

III. SUMMARY

With the aim of studying the α-cluster structure of ^{43}Sc, we have applied the microscopic $\alpha+^{39}$K cluster model. In the low-lying negative-parity states, the calculated energy spectra and electromagnetic transitions are in qualitative agreement with experiment. This may be due to strong spin-orbit splitting of fp-shell orbits and therefore the inclusion of $(fp)^3$ configurations other than (90) would be important to improve the agreement. The negative-parity $\alpha+^{39}\mathrm{K}(3/2^+)$ cluster band is predicted to start slightly above the α-threshold. There has been reported no experimental counterpart to this band. It is of importance to search for the members of the band in experiment.

On the other hand, in the positive-parity states the calculated energies and electromagnetic transition rates are in very good agreement with the observed values. The lowest band can be interpreted in terms of weak coupling scheme built on $\alpha+^{39}\mathrm{K}(3/2^+)$. The measured $E2$ transitions between these states, which show strong enhancement comparable to those of the α-cluster band in ^{40}Ca and ^{44}Ti, are well reproduced by the present model. Furthermore, interesting selectivities for $M1$ and $E1$ transitions have been understood from the viewpoint of cluster structure. The excited $\alpha+^{39}\mathrm{K}(1/2^+)$ band is predicted to start from the $1/2_2^+$ state. The observed $1/2_2^+(2.65)$ state is a good candidate for this state. It is concluded that the positive-parity α-cluster states persist in nucleus ^{43}Sc in spite of the strong spin-orbit force. Experimental studies using α-transfer reactions are desired in order to test directly the predicted α-spectroscopic factors.

ACKNOWLEDGMENTS

This work was done as a part of the research project ''α-cluster structure and $8p$-nh states in the ^{44}Ti region'' organized by the Research Center for Nuclear Physics, Osaka University in 1994. The authors are greatly indebted to the members of the projects.

[1] F. Michel, G. Reidemeister, and S. Ohkubo, Phys. Rev. Lett. **57**, 1215 (1986); Phys. Rev. C **37**, 292 (1988).
[2] S. Ohkubo, Phys. Rev. C **38**, 2377 (1988); S. Ohkubo and K. Umehara, Prog. Theor. Phys. **80**, 598 (1988).
[3] G. Reidemeister, S. Ohkubo, and F. Michel, Phys. Rev. C **41**, 63 (1990).
[4] K. F. Pal and R. G. Lovas, Phys. Lett. **96B**, 19 (1980).
[5] K. Itonaga, Prog. Theor. Phys. **66**, 2103 (1981).
[6] T. Wada and H. Horiuchi, Phys. Rev. C **38**, 2063 (1988).
[7] A. C. Merchant, J. Phys. G **10**, 885 (1984); Phys. Rev. C **36**, 778 (1987); **37**, 414 (1988); A. C. Merchant, K. F. Pal, and P. E. Hodgson, J. Phys. G **15**, 601 (1989).
[8] T. Sakuda and S. Ohkubo, Phys. Rev. C **49**, 149 (1994); **51**, 586 (1995).
[9] T. Yamaya, S. Oh-ami, M. Fujiwara, T. Itahashi, K. Katori, M. Tosaki, S. Kato, S. Hatori, and S. Ohkubo, Phys. Rev. C **42**, 1935 (1990); **41**, 2421 (1990).
[10] T. Yamaya, S. Ohkubo, S. Okabe, and M. Fujiwara, Phys. Rev. C **47**, 2389 (1993).
[11] T. Yamaya, M. Saito, M. Fujiwara, T. Itahashi, K. Katori, T. Suehiro, S. Kato, S. Hatori, and S. Ohkubo, Phys. Lett. B **306**, 1 (1993); Nucl. Phys. **A573**, 154 (1994).
[12] C. Y. Kim, and T. Udagawa, Phys. Rev. C **46**, 532 (1992); P. Guazzoni, M. Jaskola, L. Zetta, C. Y. Kim, T. Udagawa, and G. Bohlen, Nucl. Phys. **A564**, 452 (1993); Phys. Rev. C **2**, 186 (1970).
[13] T. Sakuda and F. Nemoto, Prog. Theor. Phys. **62**, 1274 (1979); **62**, 1606 (1979).
[14] I. P. Johnstone, Nucl. Phys. **A110**, 429 (1968); I. P. Johnstone and G. L. Payne, *ibid.* **A124**, 217 (1969).
[15] A. Arima, H. Horiuchi, and T. Sebe, Phys. Lett. **24B**, 129 (1967).
[16] H. Hasegawa and S. Nagata, Prog. Theor. Phys. **45**, 1786 (1971); Y. Yamamoto, *ibid.* **52**, 471 (1974).
[17] P. M. Endt, Nucl. Phys. **A521**, 1 (1990); At. Data Nucl. Data Tables **23**, 3 (1979).
[18] H. M. Sheppard, P. A. Butler, R. Daniel, P. J. Nolan, N. R. F. Rammo, and J. F. Sharpey-Schafer, J. Phys. G **6**, 511 (1980).
[19] J. B. McGrory, Phys. Rev. C **8**, 693 (1973).
[20] P. A. Smith and R. J. Peterson, Nucl. Phys. **A363**, 287 (1981).
[21] T. Motoba and K. Itonaga, Prog. Theor. Phys. Suppl. **65**, 136 (1976).
[22] T. Yamada, Phys. Rev. C **42**, 1432 (1990).
[23] G. C. Ball, J. S. Forster, F. Ingebretsen, and C. F. Monahan, Nucl. Phys. **A180**, 517 (1972).
[24] S. Froneman, W. J. Naude, W. A. Richter, J. A. Stander, and J. W. Koen, Z. Phys. A **327**, 469 (1987).
[25] E. Dafni, H. E. Mahnke, J. W. Noe, M. H. Rafailovich, and G. D. Sprouse, Phys. Rev. C **23**, 1612 (1981).
[26] J. Styczen, J. Chevallier, B. Haas, N. Schulz, P. Taras, and M. Toulemonde, Nucl. Phys. **A262**, 317 (1976).
[27] R. J. Mitchell, T. V. Ragland, R. P. Scharenberg, R. E. Holland, and F. J. Lynch, Phys. Rev. C **16**, 1605 (1977).